On the analytic solution of magnetohydrodynamic flows of non-Newtonian fluids over a stretching sheet

By SHI-JUN LIAO

School of Naval Architecture and Ocean Engineering, Shanghai Jiao Tong University,
Shanghai 200030, China
sjliao@sjtu.edu.cn

A powerful, easy-to-use analytic technique for nonlinear problems, the homotopy analysis method, is employed to give analytic solutions of magnetohydrodynamic viscous flows of non-Newtonian fluids over a stretching sheet. For the so-called second-order and third-order power-law fluids, the explicit analytic solutions are given by recursive formulas with constant coefficients. Also, for real power-law index and magnetic field parameter in a quite large range, an analytic approach is proposed. All of our analytic results agree well with numerical ones. In particular, a simple analytic formula of the dimensionless velocity gradient at the wall is found, which is accurate for all real power-law indices and magnetic field parameters. This analytic formula can give sufficiently accurate results for the skin friction on the moving sheet that it would find wide application in industries. Physically, they indicate that the magnetic field tends to increase the skin friction, and that this effect is more pronounced for shear-thinning than for shear-thickening fluids.

1. Introduction

Investigations of boundary layer flows of viscous fluid due to a stretching sheet have important practical applications in chemical and metallurgy industries. To the best of the author's knowledge, it was first studied by Sakiadis (1961) and then followed by many other researchers such as Erickson, Fan & Fox (1966), Crane (1970), McCormack & Crane (1973), McLeod & Rajagopal (1987). The boundary-layer flows of non-Newtonian fluids due to a stretching plane were investigated by Rajagopal, Na & Gupta (1984, 1987), Troy *et al.* (1987), Dandapat & Gupta (1989), Andersson & Dandapat (1991). Viscous flows due to a moving sheet in electronic-magnetic fields, i.e. magnetodhydrodynamic (MHD) flows, are relevant to many practical applications in the metallurgy industry, such as the cooling of continuous strips and filaments drawn through a quiescent fluid and the purification of molten metals from non-metallic inclusions. MHD flows of Newtonian fluids were investigated by Pavlov (1974), Chakrabarti & Gupta (1979), Vajravelu (1986), Takhar, Raptis & Perdikis (1987), Andersson (1992, 1995). To the author's knowledge, MHD flows of non-Newtonian fluids were first studied by Sarpkaya (1961) and then followed by Djukic (1973, 1974), Andersson, Bech & Dandapat (1992), etc.

Consider the flow of an electrically conducting fluid, obeying the power-law model in the presence of a transverse magnetic field, past a flat sheet lying on the plane $y = 0$, the flow being confined to $y > 0$. Two equal and opposite forces are applied

along the x-axis so that the wall is stretched keeping the origin fixed. The boundary layer flow is governed by

$$\frac{\partial u}{\partial x} + \frac{\partial v}{\partial y} = 0, \tag{1}$$

$$u\frac{\partial u}{\partial x} + v\frac{\partial u}{\partial y} = \frac{1}{\rho}\frac{\partial \tau_{xy}}{\partial y} - \left(\frac{\sigma B_0^2}{\rho}\right)u, \tag{2}$$

where u and v are velocity components in the x- and y-directions, ρ, σ, B_0 and $\tau_{x,y}$ are the density, electrical conductivity, magnetic field and shear stress, respectively. The shear stress tensor is defined by the Ostwald–de-Wäle model

$$\tau_{ij} = 2K(2D_{kl}D_{kl})^{(\kappa-1)/2}D_{i,j}, \tag{3}$$

where

$$D_{ij} = \frac{1}{2}\left(\frac{\partial u_i}{\partial x_j} + \frac{\partial u_j}{\partial x_i}\right)$$

denotes the stretching tensor, K is the consistency coefficient and κ is the power-law index. The boundary conditions are

$$u = Cx, \quad v = 0 \quad \text{at} \quad y = 0 \tag{4}$$

and

$$u \to 0 \quad \text{as} \quad y \to +\infty, \tag{5}$$

where C is a positive constant. Under the transformation

$$\psi = \left(\frac{K/\rho}{C^{1-2\kappa}}\right)^{1/(\kappa+1)} x^{2\kappa/(\kappa+1)} F(\xi) \tag{6}$$

and

$$\xi = y\left(\frac{C^{2-\kappa}}{K/\rho}\right)^{1/(\kappa+1)} x^{(1-\kappa)/(1+\kappa)}, \tag{7}$$

where

$$u = \frac{\partial \psi}{\partial y}, \qquad v = -\frac{\partial \psi}{\partial x}$$

define the stream function ψ, the governing equation becomes

$$\kappa\left[-F''(\xi)\right]^{\kappa-1} F'''(\xi) + \left(\frac{2\kappa}{\kappa+1}\right) F(\xi) F''(\xi) - F'^2(\xi) - M F'(\xi) = 0, \tag{8}$$

subject to the boundary conditions

$$F(0) = 0, \qquad F'(0) = 1, \qquad F'(+\infty) = 0, \tag{9}$$

where the prime denotes differentiation with respect to ξ and $M = \sigma B_0^2/(\rho C)$ is the magnetic parameter. The skin friction coefficient C_f at the wall is given by

$$C_f = \frac{\tau_w}{\frac{1}{2}\rho(Cx)^2} = 2[-F''(0)]^\kappa \left[\frac{(Cx)^{2-\kappa}x^\kappa}{K/\rho}\right]^{-1/(1+\kappa)}, \tag{10}$$

where $(Cx)^{2-\kappa}x^\kappa/(K/\rho)$ is the local Reynolds number based on the sheet velocity Cx. For details refer to Andersson *et al.* (1992).

Andersson *et al.* (1992) numerically solved the nonlinear differential equations (8) and (9) for seven values of the power-law index in the range $0.4 \leqslant \kappa \leqslant 2$ and

for five different values of the magnetic field $0 \leqslant M \leqslant 2$. However, to the best of the author's knowledge, no analytic results have been reported for κ and M in general cases. In this paper, an analytic tool for nonlinear problems, namely the homotopy analysis method (HAM) (Liao 1992), is employed to solve the nonlinear differential equations (8) and (9). The homotopy analysis method is based on a basic concept in topology, i.e. homotopy (Hilton 1953) that is widely applied in numerical techniques (Alexander & Yorke 1978; Chan & Keller 1982; Dinar & Keller 1985; Grigolyuk & Shalashilin 1991). Unlike perturbation techniques (Cole 1958; Van Dyke 1975; Hinch 1991; Murdock 1991; Nayfeh 2000), the homotopy analysis method is independent of small/large parameters. Unlike all other reported perturbation and non-perturbation techniques such as the artificial small parameter method (Lyapunov 1892), the δ-expansion method (Karmishin, Zhukov & Kolosov 1990; Awrejcewicz, Andrianov & Manevitch 1998) and Adomian's (1976, 1994) decomposition method, the homotopy analysis method provides us with a simple way to adjust and control the convergence region and rate of approximation series. The homotopy analysis method has been successfully applied to many nonlinear problems such as viscous flows (Liao 1999*a*,*b*), heat transfer (Liao & Campo 2002; Wang *et al.* 2003), nonlinear oscillations (Liao & Chwang 1998), nonlinear water waves (Liao & Cheung 2003), Thomas-Fermi's atom model (Liao 2003), etc. In particular, by means of the homotopy analysis method, the author (Liao 2002) gave a drag formula for a sphere in a uniform stream, which agrees well with experimental results in a considerably larger region of Reynolds number than those of all reported analytic drag formulas. All of these successful applications of the homotopy analysis method verify its validity for nonlinear problems in science and engineering.

In this paper we now employ the homotopy analysis method to solve the MHD viscous flows of non-Newtonian fluids and propose analytic solutions of (8) and (9) for $\kappa > 0$ and $0 \leqslant M \leqslant 1000$.

2. Analytic solutions for integer power-law index

Physically, the power-law index κ is a positive real number. First, let us consider the case that κ is a positive integer. When $\kappa = 1$, equation (8) becomes

$$F'''(\xi) + F(\xi)\,F''(\xi) - F'^2(\xi) - M\,F'(\xi) = 0. \tag{11}$$

This equation has an exact analytic solution (see Pavlov 1974)

$$F(\xi) = \frac{1 - \exp(-\sqrt{1 + M}\,\xi)}{\sqrt{1 + M}}, \tag{12}$$

which gives

$$F'(\xi) = \exp(-\sqrt{M + 1}\,\xi) \tag{13}$$

and

$$F''(0) = -\sqrt{1 + M}. \tag{14}$$

When $\kappa = 2$, equation (8) is

$$-2\,F''(\xi)\,F'''(\xi) + \left(\tfrac{4}{3}\right) F(\xi)\,F''(\xi) - F'^2(\xi) - M\,F'(\xi) = 0, \tag{15}$$

and when $\kappa = 3$,

$$3[F''(\xi)]^2\,F'''(\xi) + \left(\tfrac{3}{2}\right) F(\xi)\,F''(\xi) - F'^2(\xi) - M\,F'(\xi) = 0. \tag{16}$$

The zero-order deformation equation

Let λ denote a positive constant. Due to the boundary conditions (9) and the known exact solution (12) for $\kappa = 1$, $F(\xi)$ for any a positive integer κ can be expressed by a set of base functions

$$\{\exp(-n\,\lambda\,\xi) \mid n \geqslant 0\} \tag{17}$$

in the following form:

$$F(\xi) = a_0 + \sum_{n=1}^{+\infty} a_n \, \exp(-n\,\lambda\,\xi), \tag{18}$$

where a_n is a coefficient. Then, from the above expression and the boundary conditions (9), it is straightforward to choose

$$F_0(\xi) = \frac{[1 - \exp(-\lambda\,\xi)]}{\lambda} \tag{19}$$

as the initial guess of $F(\xi)$. Also, due to (18) and the governing equation (8), we choose

$$\mathscr{L}[\Phi(\xi;q)] = \frac{\partial^3 \Phi(\xi;q)}{\partial \xi^3} - \lambda^2 \, \frac{\partial \Phi(\xi;q)}{\partial \xi}, \tag{20}$$

as our auxiliary linear operator, where q is an embedding parameter. Note that the auxiliary linear operator $\mathscr{L}$ has the property

$$\mathscr{L}\left[C_1 + C_2 \exp(-\lambda\,\xi) + C_3 \, \exp(\lambda\,\xi)\right] = 0. \tag{21}$$

Furthermore, we define using (8) the nonlinear operator

$$\mathscr{N}[\Phi(\xi;q)] = \kappa \left[-\frac{\partial^2 \Phi(\xi;q)}{\partial \xi^2}\right]^{\kappa-1} \frac{\partial^3 \Phi(\xi;q)}{\partial \xi^3} + \left(\frac{2\kappa}{\kappa+1}\right) \Phi(\xi;q) \frac{\partial^2 \Phi(\xi;q)}{\partial \xi^2}$$
$$- \left[\frac{\partial \Phi(\xi;q)}{\partial \xi}\right]^2 - M \frac{\partial \Phi(\xi;q)}{\partial \xi}, \quad (22)$$

where κ is a positive integer. Then, we construct the zero-order deformation equation

$$(1-q)\,\mathscr{L}\,[\Phi(\xi;q) - F_0(\xi)] = \hbar\,q\,\exp(-l\lambda\,\xi)\,\mathscr{N}\,[\Phi(\xi;q)], \qquad q \in [0,1], \tag{23}$$

subject to the boundary conditions

$$\Phi(0;q) = 0, \qquad \frac{\partial \Phi(\xi;q)}{\partial \xi}\bigg|_{\xi=0} = 1, \qquad \frac{\partial \Phi(\xi;q)}{\partial \xi}\bigg|_{\xi=+\infty} = 0. \tag{24}$$

When $q = 0$, it is straightforward to show that the solution of (23) and (24) is

$$\Phi(\xi;0) = F_0(\xi). \tag{25}$$

When $q = 1$, equations (23) and (24) are respectively the same as (8) and (9), provided

$$\Phi(\xi;1) = F(\xi). \tag{26}$$

Thus, as q increases from 0 to 1, $\Phi(\xi;q)$ varies from the initial guess $F_0(\xi)$, defined by (19), to the exact solution $F(\xi)$ governed by (8) and (9). This kind of continuous variation is called deformation in topology.

Using (25), it is straightforward to expand $\Phi(\xi;q)$ in a power series of the embedding parameter q as follows:

$$\Phi(\xi;q) = F_0(\xi) + \sum_{m=1}^{+\infty} F_m(\xi)\, q^m, \qquad (27)$$

where

$$F_m(\xi) = \frac{1}{m!} \left. \frac{\partial^m \Phi(\xi;q)}{\partial q^m} \right|_{q=0}. \qquad (28)$$

Note that the zero-order deformation equation (23) contains a non-zero auxiliary parameter $\hbar$. Thus, $\Phi(\xi;q)$ and $F_m(\xi)$ are dependent upon this parameter. Obviously, $\hbar$ also affects the convergence rate and region of the series (27). Assume that $\hbar$ is chosen so that the series (27) is convergent at $q = 1$. Then, due to (26) and (27), we have the relationship

$$F(\xi) = F_0(\xi) + \sum_{m=1}^{+\infty} F_m(\xi). \qquad (29)$$

The high-order deformation equation

Differentiating the zero-order deformation equations (23) and (24) m times with respect to q and then dividing them by $m!$ and finally setting $q = 0$, we have, due to the definition (28), the mth-order deformation equation

$$\mathscr{L}\left[F_m(\xi) - \chi_m\, F_{m-1}(\xi)\right] = \hbar\, \exp(-l\lambda\,\xi)\, R_m(\xi), \qquad (30)$$

subject to the boundary conditions

$$F_m(0) = 0, \qquad F_m'(0) = 0, \qquad F_m'(+\infty) = 0, \qquad (31)$$

where

$$R_m(\xi) = \frac{1}{(m-1)!} \left. \frac{\partial^{m-1} \mathscr{N}[\Phi(\xi;q)]}{\partial q^{m-1}} \right|_{q=0} \qquad (32)$$

and

$$\chi_m = \begin{cases} 0 & \text{when } m \leqslant 1, \\ 1 & \text{when } m \geqslant 2. \end{cases} \qquad (33)$$

Note that $R_m(\xi)$ is dependent upon the integer power-law index κ. When $\kappa = 1$, we have

$$R_m(\xi) = F_{m-1}'''(\xi) + \sum_{n=0}^{m-1} \left[F_n(\xi)\, F_{m-1-n}''(\xi) - F_n'(\xi)\, F_{m-1-n}'(\xi) \right] - M\, F_{m-1}'(\xi). \qquad (34)$$

When $\kappa = 2$,

$$R_m(\xi) = \sum_{n=0}^{m-1} \left[4 F_n(\xi)\, F_{m-1-n}''(\xi)/3 - F_n'(\xi)\, F_{m-1-n}'(\xi) \right]$$

$$- M F_{m-1}'(\xi) - 2 \sum_{n=0}^{m-1} F_n''(\xi)\, F_{m-1-n}'''(\xi). \qquad (35)$$

When $\kappa = 3$,

$$R_m(\xi) = \sum_{n=0}^{m-1} \left[3F_n(\xi) \, F''_{m-1-n}(\xi)/2 - F'_n(\xi) \, F'_{m-1-n}(\xi)\right] - M \, F'_{m-1}(\xi)$$

$$+3\sum_{n=0}^{m-1}\sum_{j=0}^{n} F''_j(\xi) \, F''_{n-j}(\xi) \, F'''_{m-1-n}(\xi). \quad (36)$$

Note also that $R_m(\xi)$ contains the term $\exp(-\lambda \, \xi)$. It is found that, when $l = 0$, the right-hand side of equation (30) contains the term $\exp(-\lambda \, \xi)$. Then, due to (21), the solution of equation (30) has the term

$$\xi \, \exp(-\lambda \, \xi),$$

which disobeys expression (18) however. So, in order to obey (18), we have to choose $l \geqslant 1$. On the other hand, it is found that, when $l \geqslant 2$, the solution of (30) does not contain the term

$$\exp(-2\lambda \, \xi),$$

so that the coefficient of the term $\exp(-2\lambda \, \xi)$ cannot be further improved even if $m \to +\infty$. To avoid both these difficulties, we must have

$$l = 1. \qquad (37)$$

It should be emphasized that we still have freedom to choose a positive value for λ and a negative value for the auxiliary parameter $\hbar$. For simplicity we choose $\lambda = 1$ in this section for the integer power-law index κ. We will show that the auxiliary parameter $\hbar$ plays an important role in the homotopy analysis method.

2.1. Solutions when $\kappa = 1$

The exact solution (12) can be employed to verify the validity of the foregoing analytic approach. It is straightforward to solve the linear equations (30) and (31). It is found that, when $\kappa = 1$, $F_m(\xi)$ governed by (30) and (31) can be expressed by

$$F_m(\xi) = \sum_{n=0}^{2m+1} a_{m,n} \, \exp(-n \, \lambda \, \xi), \qquad (38)$$

where $a_{m,n}$ is a coefficient. Substituting (38) into the mth-order deformation equations (30) and (31), we have the recursive formulas

$$a_{m,n} = \chi_m \, \chi_{2m+1-n} \, a_{m-1,n} + \frac{\hbar \, \chi_{2m+2-n} \, (n-1) \, [\lambda^2 \, (n-1)^2 - M] \, a_{m-1,n-1}}{\lambda^2 n \, (n^2 - 1)}$$

$$- \frac{\hbar \, (A_{m,n-1} - \chi_{n-1} \, B_{m,n-1})}{\lambda \, n \, (n^2 - 1)} \quad (39)$$

for $2 \leqslant n \leqslant 2m + 1$ and

$$a_{m,1} = -\sum_{n=2}^{2m+1} n \, a_{m,n}, \qquad (40)$$

$$a_{m,0} = -\sum_{n=1}^{2m+1} a_{m,n} \qquad (41)$$

under the definitions

$$A_{m,j} = \sum_{n=0}^{m-1} \sum_{i=\max\{0,j-2m+2n+1\}}^{\min\{2n+1,j-1\}} (j-i)^2 \, a_{n,i} \, a_{m-n-1,j-i}, \quad 1 \leqslant j \leqslant 2m \tag{42}$$

and

$$B_{m,j} = \sum_{n=0}^{m-1} \sum_{i=\max\{1,j-2m+2n+1\}}^{\min\{2n+1,j-1\}} i(j-i) \, a_{n,i} \, a_{m-n-1,j-i}, \quad 2 \leqslant j \leqslant 2m. \tag{43}$$

Due to the initial guess (19), we have the first two coefficients:

$$a_{0,0} = 1/\lambda, \qquad a_{0,1} = -1/\lambda. \tag{44}$$

Thus, starting from these two coefficients, we can calculate the coefficients $a_{m,n}$ for $m = 1, 2, 3, \ldots, 0 \leqslant n \leqslant 2m + 1$ by means of the above recursive formulas. So, we have the explicit analytic solution

$$F(\xi) = \sum_{k=0}^{+\infty} \sum_{n=0}^{2k+1} a_{k,n} \, \exp(-n \, \lambda \, \xi) \tag{45}$$

for the Newtonian fluid. At the mth-order of approximation we have

$$F(\xi) \approx \sum_{k=0}^{m} \sum_{n=0}^{2k+1} a_{k,n} \, \exp(-n \, \lambda \, \xi), \tag{46}$$

which gives

$$F'(\xi) \approx -\lambda \sum_{k=0}^{m} \sum_{n=1}^{2k+1} n \, a_{k,n} \, \exp(-n \, \lambda \, \xi), \tag{47}$$

$$F''(0) \approx \lambda^2 \sum_{k=0}^{m} \sum_{n=1}^{2k+1} n^2 \, a_{k,n}. \tag{48}$$

It is found that when $\kappa = 1$ the mth-order approximation of $F''(0)$ can be expressed by

$$F''(0) \approx \sum_{n=0}^{m} \alpha_1^{m,n} \, M^n, \tag{49}$$

where $\alpha_1^{m,n}$ is coefficient dependent upon $\hbar$. Thus, our results contain an auxiliary parameter $\hbar$, which plays an important role in the homotopy analysis method. As verified in the author's previous publications (Liao & Chwang 1998; Liao 1999 *a*,*b*, 2003; Liao & Campo 2002; Liao & Cheung 2003), it is the value of the auxiliary parameter $\hbar$ which can adjust and control the convergence region and rate of the series given by the homotopy analysis method. It is found that the convergence region of above series increases as $\hbar$ tends to zero from below, as shown in figure 1.

A power series of $F''(0)$ can be obtained by expanding the exact solution (14) as follows:

$$F''(0) \approx 1 + \frac{M}{2} - \frac{M^2}{8} + \frac{M^3}{16} - \frac{5M^4}{128} + \cdots, \tag{50}$$

which is convergent in a rather restricted region $0 \leqslant M < 2$ however, as shown in figure 1. Employing the traditional Padé technique to the above power series of the
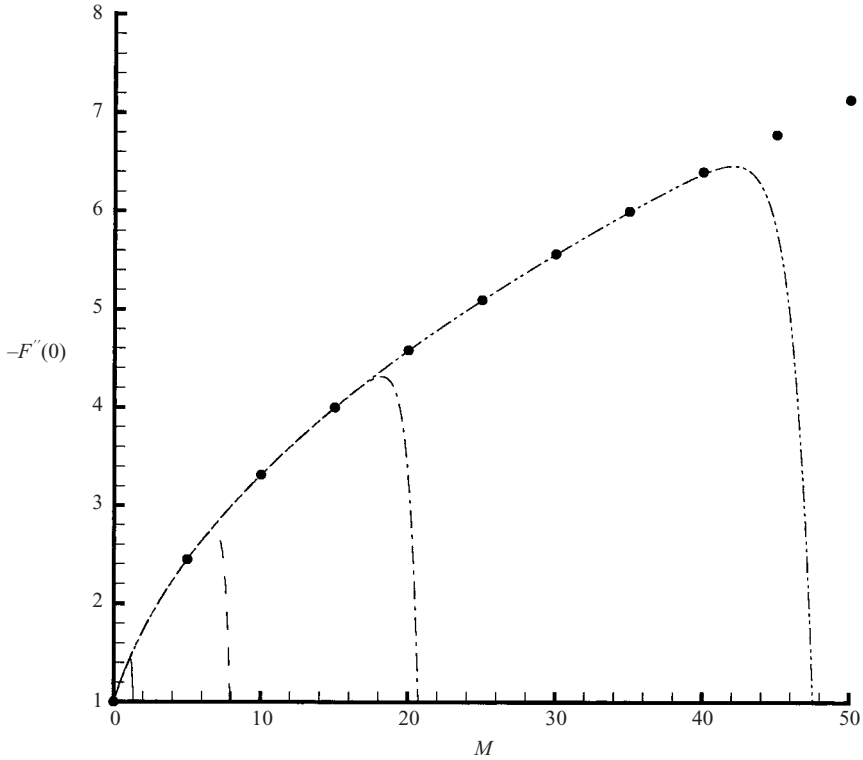
FIGURE 1. Comparison of $F''(0)$ at the 20th-order of approximation given by the homotopy analysis method with the exact solution (14) and perturbation result (50) when $\kappa = 1$. Symbols: exact solution (14); solid line: perturbation result (50); dashed line: homotopy analysis approximation when $\hbar = -1$; dash-dotted line: homotopy analysis approximation when $\hbar = -1/2$; dash-dot-dotted line: homotopy analysis approximation when $\hbar = -1/4$.

physical parameter M, one has the $[m, m]$ Padé approximant

$$F''(0) \approx -\frac{1 + \sum\limits_{n=1}^{m} \delta_{m,n}\, M^n}{1 + \sum\limits_{n=1}^{m} \delta_{m,m+n}\, M^n}, \tag{51}$$

where $\delta_{m,n}$ is constant. Recently, Liao & Cheung (2003) proposed a so-called homotopy-Padé method, which is more efficient than the traditional Padé approximant. From (27), we have the $(2m)$th-order approximation

$$\left.\frac{\partial^2 \Phi(\xi\,;q)}{\partial \xi^2}\right|_{\xi=0} \approx \sum_{n=0}^{2m} F_n''(0)\, q^n. \tag{52}$$

Employing the traditional Padé technique to the power series of the embedding parameter q, we have the $[m, m]$ Padé approximant

$$\left.\frac{\partial^2 \Phi(\xi\,;q)}{\partial \xi^2}\right|_{\xi=0} \approx -\frac{1 + \sum\limits_{n=1}^{m} \gamma_{m,n}\, q^n}{1 + \sum\limits_{n=1}^{m} \gamma_{m,m+n}\, q^n}, \tag{53}$$
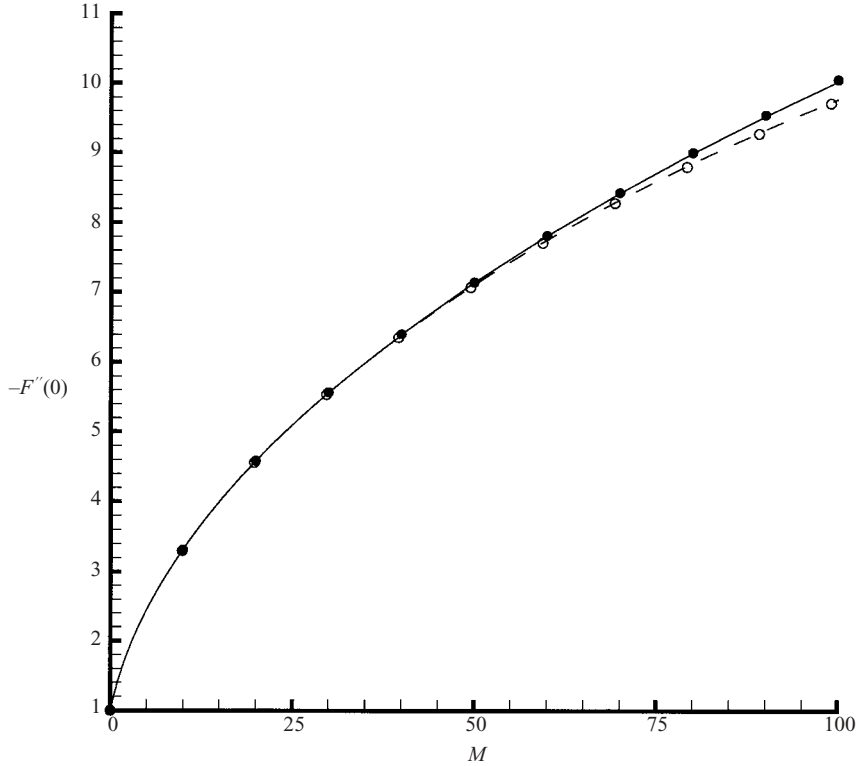
FIGURE 2. Comparison of $F''(0)$ given by the homotopy-Padé method with the exact solution (14) and the traditional Padé technique when $\kappa = 1$. Filled circles: exact solution (14); open circles: traditional [10,10] Padé approximation; dashed line: [4,4] homotopy-Padé approximation; solid line: [6,6] homotopy-Padé approximation.

where $\gamma_{m,n}$ is a coefficient. Setting $q = 1$ in above series, we obtain using (29) that

$$F''(0) \approx -\frac{1 + \sum_{n=1}^{m} \gamma_{m,n}}{1 + \sum_{n=1}^{m} \gamma_{m,m+n}}. \tag{54}$$

It is found that the above $[m, m]$ homotopy-Padé expression can be rewritten as

$$F''(0) \approx -\frac{1 + \sum_{n=1}^{m^2} \Delta_1^{m,n} M^n}{1 + \sum_{n=1}^{m^2} \Delta_1^{m,m^2+n} M^n}, \tag{55}$$

where $\Delta_1^{m,n}$ $(1 \leqslant n \leqslant 2m^2)$ is constant, which is found to be independent of the auxiliary parameter $\hbar$. Note that the traditional Padé approximant analyses results expressed by physical parameters, which have been obtained by setting $q = 1$. However, in the homotopy-Padé method, one first analyses the power series in the embedding parameter q and then sets $q = 1$. This is the distinction between the traditional Padé approximant and the homotopy-Padé ones. It is interesting that the above $[m, m]$ homotopy-Padé approximant contains the term M^{m^2} while the traditional $[m, m]$ Padé approximant (51) has only the term M^m. As shown in figure 2, even

n	Padé approximant	Homotopy-Padé approximant
1	2.42857	3.08333
2	3.03390	3.30134
3	3.23265	3.31605
4	3.92217	3.31661
5	3.30958	3.31662
6	3.31459	3.31662
8	3.31646	3.31662
10	3.31661	3.31662

TABLE 1. Comparison of the $[n, n]$ homotopy-Padé approximant of $-F''(0)$ with the traditional $[n, n]$ Padé approximant when $\kappa = 1$ and $M = 10$.
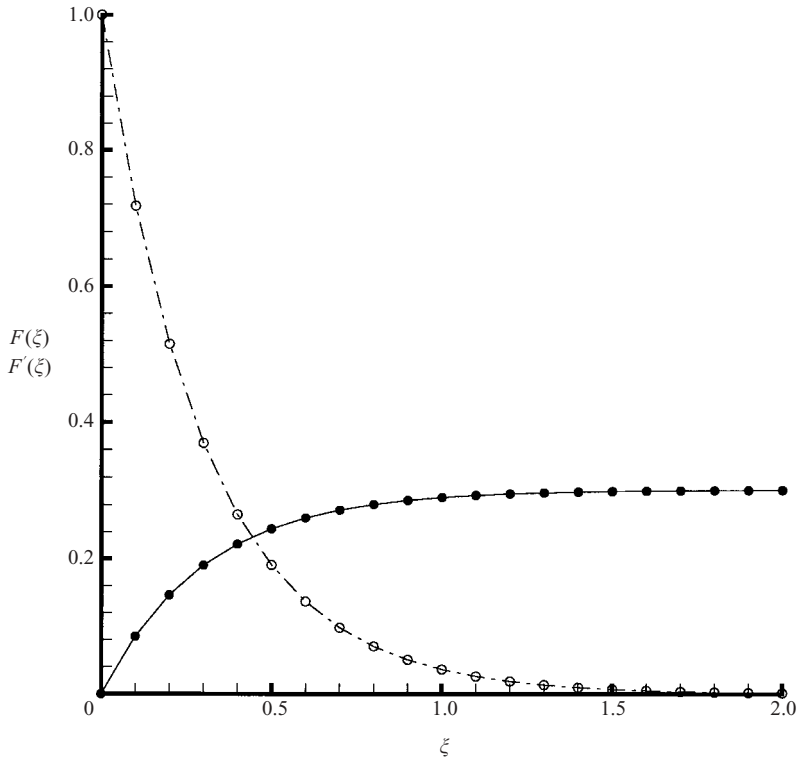

FIGURE 3. Comparison of $F(\xi)$ and $F'(\xi)$ given by the homotopy-Padé technique with the exact solution (12) and (13) when $\kappa = 1$ and $M = 10$. Filled circles: exact solution (12); open circles: exact solution (13); solid line: [5,5] homotopy-Padé approximation of $F(\xi)$; dashed line: [5,5] homotopy-Padé approximation of $F'(\xi)$.

the [4,4] homotopy-Padé approximant gives as accurate an approximation as the traditional [10, 10] Padé approximant and the [6,6] homotopy-Padé approximant agrees well with the exact result. Clearly, the homotopy-Padé approximant of $-F''(0)$ converges much faster to the exact result $\sqrt{1 + M}$ than the traditional Padé technique, as shown in table 1 and figures 1 and 2. Similarly, one can employ the homotopy-Padé technique to obtain more accurate results of $F(\xi)$ and $F'(\xi)$. For example, when $M = 10$, the [5,5] homotopy-Padé approximants of $F(\xi)$ and $F'(\xi)$ agree well with the exact solutions (12) and (13), respectively, as shown in figure 3. It is interesting that

the numerator and denominator of the homotopy-Padé approximants of $F(\xi)$ and $F'(\xi)$ are sums of exponential functions of ξ. All of these clearly verify the validity of the proposed analytic approach and the homotopy-Padé method, although the exact solution is known when $\kappa = 1$.

2.2. *Solutions when $\kappa = 2$*

For the second-order power-law fluid ($\kappa = 2$), it is found that $F_m(\xi)$ governed by (30) and (31) can be expressed by

$$F_m(\xi) = \sum_{n=0}^{2m+1} a_{m,n} \exp(-n \lambda \xi). \tag{56}$$

Substituting this into the mth-order deformation equations (30) and (31), we have the recursive formula

$$a_{m,n} = \chi_m \chi_{2m+1-n} a_{m-1,n} - \frac{\hbar \chi_{2m+2-n} M a_{m-1,n-1}}{\lambda^2 n (n+1)}$$
$$- \frac{\hbar (4A_{m,n-1}/3 - \chi_{n-1} B_{m,n-1})}{\lambda n (n^2 - 1)} - \frac{2 \hbar \lambda^2 \chi_{n-1} C_{m,n-1}}{n (n^2 - 1)} \tag{57}$$

for $2 \leqslant n \leqslant 2m + 1$, and

$$a_{m,1} = -\sum_{n=2}^{2m+1} n\, a_{m,n}, \tag{58}$$

$$a_{m,0} = -\sum_{n=1}^{2m+1} a_{m,n}, \tag{59}$$

where

$$C_{m,j} = \sum_{n=0}^{m-1} \sum_{i=\max\{1, j-2m+2n+1\}}^{\min\{2n+1, j-1\}} i^2 (j-i)^3 a_{n,i} a_{m-n-1, j-i}, \quad 2 \leqslant j \leqslant 2m \tag{60}$$

and $A_{m,n}$, $B_{m,n}$ are defined by (42) and (43), respectively. So, we have the explicit analytic solution

$$F(\xi) = \sum_{k=0}^{+\infty} \sum_{n=0}^{2k+1} a_{k,n} \exp(-n \lambda \xi) \tag{61}$$

for the second-order power-law fluid. The mth-order approximations of $F(\xi)$ and $F'(\xi)$ are the same as (46) and (47), respectively. The first two coefficients are given by (44).

It is found that when $\kappa = 2$ the mth-order approximation of $F''(0)$ can be expressed by

$$F''(0) \approx \sum_{n=0}^{m} \alpha_2^{m,n} M^n, \tag{62}$$

where $\alpha_2^{m,n}$ is a coefficient dependent upon $\hbar$. Similarly, as $\hbar$ tends to zero from below, the convergence region of $F''(0)$ enlarges. The analytic approximations of $F''(0)$ for $M = 1/2, 1, 3/2$ and 2 when $\hbar = -1/2$ are given in table 2, and they agree well with the numerical results 1.093, 1.187, 1.269 and 1.342 given by Andersson *et al.* (1992), respectively. It is found that when $\hbar = -1/(2 + M/10)$ the series of our analytic solutions converge for any a magnetic field parameter $M \geqslant 0$.

m	$M = 1/2$	$M = 1$	$M = 3/2$	$M = 2$
5	1.054	1.157	1.247	1.325
10	1.070	1.173	1.260	1.336
20	1.082	1.182	1.266	1.340
30	1.087	1.185	1.268	1.341
40	1.090	1.186	1.269	1.341
50	1.091	1.187	1.269	1.342
60	1.092	1.187	1.269	1.342
70	1.093	1.187	1.269	1.342
80	1.093	1.187	1.269	1.342

TABLE 2. The mth-order homotopy analysis solution for $-F''(0)$ when $\kappa = 2$ and $\hbar = -1/2$.

n	$M = 1/2$	$M = 1$	$M = 3/2$	$M = 2$
5	1.090	1.185	1.266	1.339
10	1.094	1.187	1.269	1.342
20	1.092	1.187	1.269	1.342
30	1.093	1.187	1.269	1.342
40	1.093	1.187	1.269	1.342

TABLE 3. The $[n, n]$ homotopy-Padé approximant of $-F''(0)$ when $\kappa = 2$.

It is straightforward to employ the traditional Padé technique to the series of $F''(0)$. It is found that this cannot enlarge convergence regions of the series (62), which are mainly determined by $\hbar$. Thus, the traditional Padé technique seems of no use when $\kappa = 2$.

Unlike the traditional Padé technique, the homotopy-Padé method can greatly increase the convergence rate and region of the series of $F''(0)$. It is found that when $\kappa = 2$ the corresponding $[m, m]$ homotopy-Padé approximant of $F''(0)$ can be expressed by

$$F''(0) \approx \frac{\Delta_2^{m,0} + \sum_{n=1}^{m^2+m} \Delta_2^{m,n} M^n}{1 + \sum_{n=1}^{m^2+m} \Delta_2^{m,m^2+m+n} M^n}, \tag{63}$$

where the constant $\Delta_2^{m,n}$ ($0 \leqslant n \leqslant 2m^2 + 2m$) is also independent of $\hbar$. Note that, unlike (55), the above expression contains the term M^{m^2+m}. By comparing table 2 with table 3, it is clear that the convergence rate can be considerably increased by the homotopy-Padé method. Also, the convergence region can be greatly enlarged. The $[5,5]$ and $[6,6]$ homotopy-Padé approximations of $F''(0)$ agree well with numerical results in the region $0 \leqslant M \leqslant 1000$, respectively, as shown in figure 4. The convergent analytic results of $F''(0)$ agree well with numerical results, as shown in table 4. This further verifies the validity of our analytic approach.

2.3. Solutions when $\kappa = 3$

For the third-order power-law fluid ($\kappa = 3$), it is found that $F_m(\xi)$ governed by (30) and (31) can be expressed by

$$F_m(\xi) = \sum_{n=0}^{3m+1} b_{m,n} \exp(-n \lambda \xi). \tag{64}$$

M	Analytic result	Numerical result	Results given by (81)
0	0.980	0.980	0.969
0.5	1.093	1.093	1.087
1	1.187	1.187	1.184
1.5	1.269	1.269	1.267
2	1.342	1.342	1.340
3	1.467	1.468	1.467
4	1.575	1.575	1.575
5	1.670	1.670	1.670
6	1.755	1.755	1.755
8	1.904	1.904	1.905
10	2.033	2.033	2.033
20	2.514	2.515	2.515
40	3.138	3.138	3.138
60	3.580	3.581	3.580
80	3.934	3.935	3.934
100	4.234	4.234	4.234
200	5.324	5.325	5.324
400	6.701	6.702	6.701
600	7.668	7.670	7.668
800	8.439	8.441	8.439
1000	9.089	9.091	9.089

TABLE 4. Comparison of the numerical results with the analytic results of $-F''(0)$ given by the homotopy-Padé technique when $\kappa = 2$.
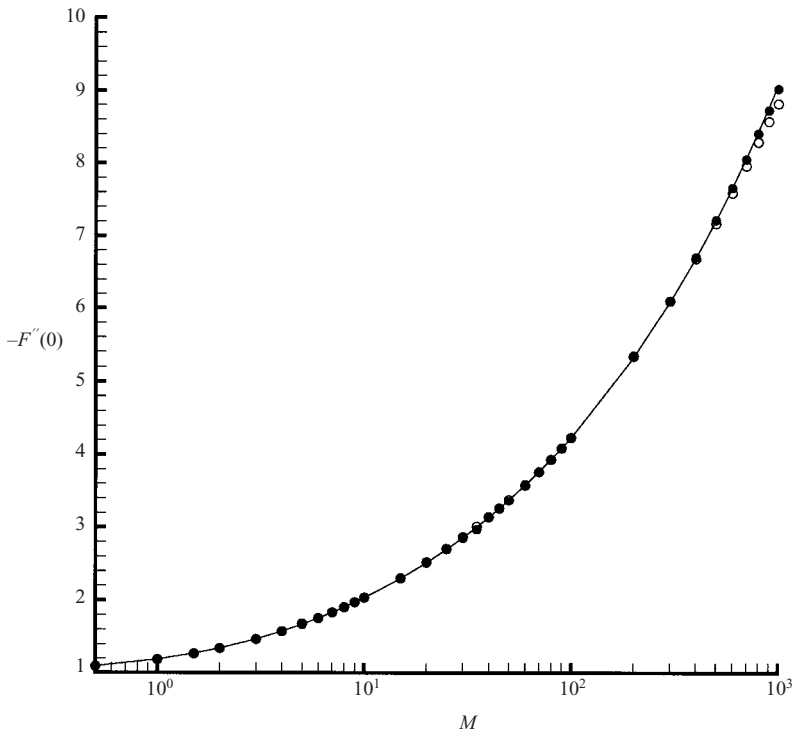

FIGURE 4. Comparison of $F''(0)$ given by the homotopy-Padé method with the numerical results when $\kappa = 2$. Solid line: numerical solution; open circle: [5,5] homotopy-Padé approximation; filled circle: [6,6] homotopy-Padé approximation.

Substituting this into the mth-order deformation equations (30) and (31), we have the recursive formula

$$b_{m,n} = \chi_m \, \chi_{3m-n} \, b_{m-1,n} - \frac{\hbar \, \chi_{3m+1-n} \, M \, b_{m-1,n-1}}{\lambda^2 n \, (n+1)}$$

$$- \frac{\hbar \, \chi_{3m+2-n} \, (3D_{m,n-1}/2 - \chi_{n-1} \, S_{m,n-1})}{\lambda \, n \, (n^2-1)} + \frac{3 \, \hbar \, \lambda^4 \, \chi_{n-2} \, Q_{m,n-1}}{n \, (n^2-1)} \quad (65)$$

for $2 \leqslant n \leqslant 3m + 1$, where

$$D_{m,j} = \sum_{n=0}^{m-1} \sum_{i=\max\{0,j-3m+3n+2\}}^{\min\{3n+1,j-1\}} (j-i)^2 \, b_{n,i} \, b_{m-n-1,j-i}, \quad 1 \leqslant j \leqslant 3m-1, \quad (66)$$

$$S_{m,j} = \sum_{n=0}^{m-1} \sum_{i=\max\{1,j-3m+3n+2\}}^{\min\{3n+1,j-1\}} i \, (j-i) \, b_{n,i} \, b_{m-n-1,j-i}, \quad 2 \leqslant j \leqslant 3m-1, \quad (67)$$

$$Q_{m,j} = \sum_{n=0}^{m-1} \sum_{i=\max\{2,j-3m+3n+2\}}^{\min\{3n+2,j-1\}} (j-i)^3 \, b_{m-n-1,j-i} \, T_{n,i}, \quad 3 \leqslant j \leqslant 3m \quad (68)$$

and

$$T_{k,j} = \sum_{n=0}^{k} \sum_{i=\max\{1,j-3k+3n-1\}}^{\min\{3n+1,j-1\}} i^2 \, (j-i)^2 \, b_{n,i} \, b_{k-n,j-i}, \quad 2 \leqslant j \leqslant 3k+2. \quad (69)$$

Also, from the boundary conditions (31), we have

$$b_{m,1} = -\sum_{n=2}^{3m+1} n \, b_{m,n}, \quad (70)$$

$$b_{m,0} = -\sum_{n=1}^{3m+1} b_{m,n}. \quad (71)$$

The initial guess (19) gives the first two coefficients as

$$b_{0,0} = 1/\lambda, \quad b_{0,1} = -1/\lambda. \quad (72)$$

Starting from these two coefficients, we can calculate the coefficients $b_{m,n}$ for $m = 1, 2, 3, \cdots, 0 \leqslant n \leqslant 3m + 1$ by means of the above recursive formulas. So, we have the explicit analytic solution

$$F(\xi) = \sum_{k=0}^{+\infty} \sum_{n=0}^{3k+1} b_{k,n} \, \exp(-n \, \lambda \, \xi) \quad (73)$$

for the third-order power-law fluid. At the mth-order of approximation we have

$$F(\xi) \approx \sum_{k=0}^{m} \sum_{n=0}^{3k+1} b_{k,n} \, \exp(-n \, \lambda \, \xi), \quad (74)$$

which gives

$$F'(\xi) \approx -\lambda \sum_{k=0}^{m} \sum_{n=1}^{3k+1} n \, b_{k,n} \, \exp(-n \, \lambda \, \xi) \quad (75)$$

and

$$F''(0) \approx \lambda^2 \sum_{k=0}^{m} \sum_{n=1}^{3k+1} n^2 \, b_{k,n}. \tag{76}$$

It is found that when $\kappa = 3$ the mth-order approximation of $F''(0)$ can be expressed by

$$F''(0) \approx \sum_{n=0}^{m} \alpha_3^{m,n} \, M^n, \tag{77}$$

where $\alpha_3^{m,n}$ is a coefficient dependent upon $\hbar$. Similarly, as $\hbar$ tends to zero from below, the convergence region of $F''(0)$ enlarges. It is found that the series converges for any $M \geqslant 0$ when $\hbar = -1/(3 + M)$ and that the convergence region of (77) cannot be enlarged by the traditional Padé technique. When $\kappa = 3$, the corresponding $[m, m]$ homotopy-Padé approximant of $F''(0)$ can be expressed by

$$F''(0) \approx \frac{\Delta_3^{m,0} + \displaystyle\sum_{n=1}^{m^2+m} \Delta_3^{m,n} \, M^n}{1 + \displaystyle\sum_{n=1}^{m^2+m} \Delta_3^{m,m^2+m+n} \, M^n}, \tag{78}$$

where the constant $\Delta_3^{m,n}$ $(0 \leqslant n \leqslant 2m^2 + 2m)$ is independent of $\hbar$. The convergence region of $F''(0)$ can be greatly enlarged by the homotopy-Padé method, as shown in figure 5. Note that the [10,10] homotopy-Padé approximant of $F''(0)$ agrees well with the numerical results in a larger region than the [5,5] homotopy-Padé approximant. It is found that the [25,25] homotopy-Padé approximants of $F''(0)$ converge in the region $0 \leqslant M \leqslant 1000$. The convergent analytic results of $F''(0)$ in the range $0 \leqslant M \leqslant 1000$ agree well with numerical results, as shown in table 5.

2.4. *A simple approximate formula for skin friction*

From the definition (10), the skin friction coefficient C_f is determined by the dimensionless velocity gradient $F''(0)$ at the wall. When $\kappa = 1$, we have the exact formula (14) for $F''(0)$, which indicates that, for large M, $\ln[-F''(0)]$ is positively proportional to $\ln M$. Our analytic results indicate that, when $\kappa = 2$ and $\kappa = 3$, $\ln[-F''(0)]$ is also positively proportional to $\ln M$, if M is large enough. This implies that

$$F''(0) \approx -(\alpha + \beta \, M)^\gamma \tag{79}$$

might be a good approximation of $F''(0)$ for any a positive integer $\kappa \geqslant 1$. Using the exact solution (14), we have

$$\alpha = 1, \quad \beta = 1, \quad \gamma = 1/2, \quad \text{when } \kappa = 1.$$

To ensure that (79) is consistent with the exact formula (14) for $\kappa = 1$, we first simply set $\alpha = 1$ for all κ. Keeping this in mind and plotting curves defined by (79), and comparing them with analytic results listed in tables 4 and 5, we find, some what surprisingly, that, if

$$\alpha = 1, \quad \beta = \frac{\kappa + 1}{2\kappa}, \quad \gamma = \frac{1}{\kappa + 1}, \tag{80}$$

the formula (79) is a very good approximation for $F''(0)$ when $\kappa = 2$ and $\kappa = 3$, especially for large M. Furthermore, it is found that even better results for $F''(0)$ are

M	Analytic result	Numerical result	Result given by (81)
0	0.985	0.985	0.975
0.5	1.060	1.060	1.055
1	1.123	1.123	1.119
1.5	1.177	1.177	1.175
2	1.224	1.224	1.223
3	1.306	1.306	1.305
4	1.374	1.375	1.375
5	1.434	1.435	1.435
6	1.488	1.488	1.488
8	1.579	1.580	1.580
10	1.658	1.658	1.659
20	1.942	1.942	1.942
40	2.291	2.291	2.291
60	2.529	2.529	2.529
80	2.713	2.714	2.714
100	2.867	2.867	2.867
200	3.404	3.404	3.404
400	4.044	4.045	4.044
600	4.475	4.475	4.475
800	4.807	4.808	4.808
1000	5.083	5.084	5.083

TABLE 5. Comparison of the numerical results with the analytic results for $-F''(0)$ given by the homotopy-Padé technique when $\kappa = 3$.
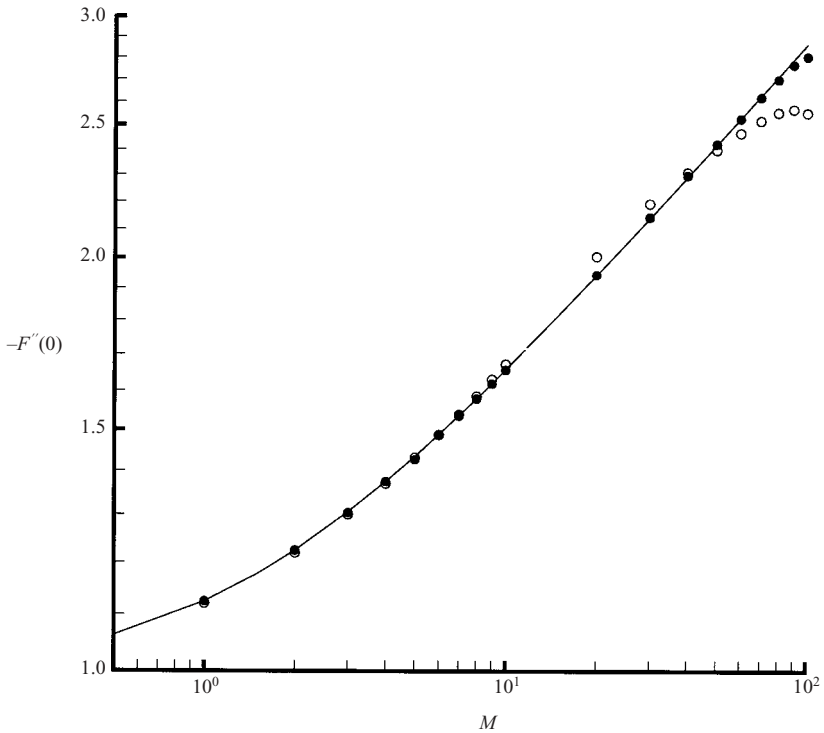

FIGURE 5. Comparison of $F''(0)$ given by the homotopy-Padé method with the numerical results when $\kappa = 3$. Solid line: numerical solution; open circle: [5,5] homotopy-Padé approximation; filled circle: [10,10] homotopy-Padé approximation.
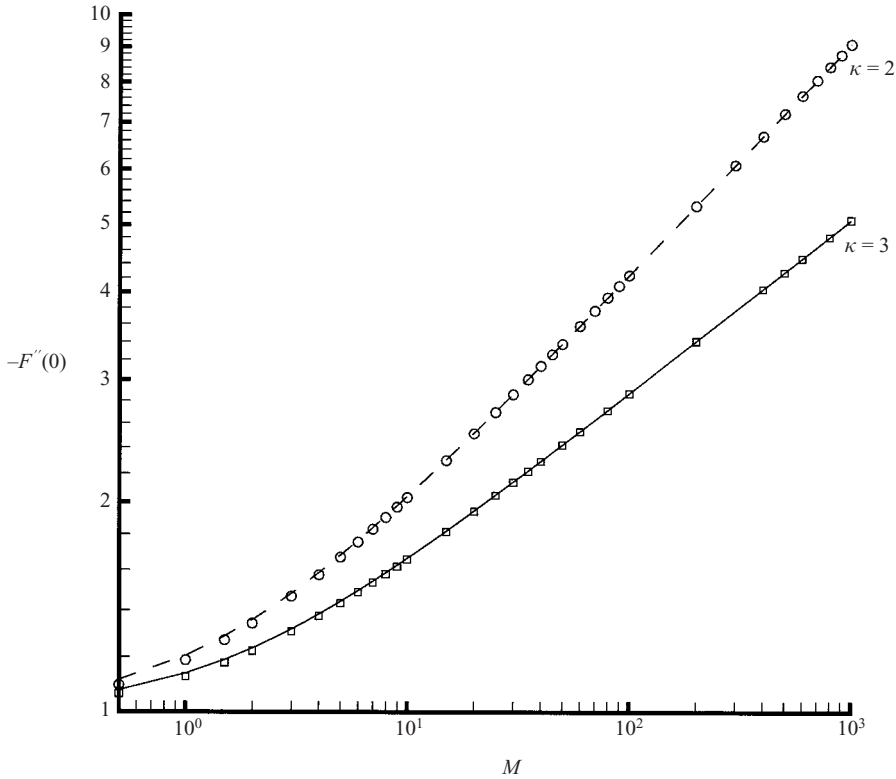
FIGURE 6. Comparison of $F''(0)$ from the approximate expression (81) with the numerical results. Dashed line: result given by (81) when $\kappa = 2$; solid line: result given by (81) when $\kappa = 3$; open circle: the numerical results when $\kappa = 2$; square: the numerical results when $\kappa = 3$.

given by choosing

$$\alpha = \left(\frac{\kappa + 1}{2\kappa}\right)^{1/(1+\kappa)},$$

i.e.

$$F''(0) \approx -\left[\left(\frac{\kappa + 1}{2\kappa}\right)^{1/(1+\kappa)} + \left(\frac{\kappa + 1}{2\kappa}\right) M\right]^{1/(\kappa+1)}, \quad (81)$$

as shown in table 4, table 5 and figure 6. When $\kappa = 2$ and $\kappa = 3$, the relative error of the above simple expression is less than 0.2% for $M \geqslant 2$. When $M \geqslant 2$, the series of approximations converge in most case, provided

$$\lambda = \left[\left(\frac{\kappa + 1}{2\kappa}\right)^{1/(1+\kappa)} + \left(\frac{\kappa + 1}{2\kappa}\right) M\right]^{1/(1+\kappa)} \quad (82)$$

and

$$\hbar = -\left[\left(\frac{\kappa + 1}{2\kappa}\right)^{1/(1+\kappa)} + \left(\frac{\kappa + 1}{2\kappa}\right) M\right]^{-1}. \quad (83)$$

In the next section we will show that the simple analytic expression (81) is valid even for real power-law index $\kappa > 0$.

3. Analytic solutions for real power-law index

The zero-order deformation equation

For real power-law index $\kappa > 0$, $F(\xi)$ can be expressed by a set of base functions

$$\{\xi^m \exp(-n\,\lambda\,\xi) \mid m \geqslant 0,\; n \geqslant 0\} \tag{84}$$

in the following form:

$$F(\xi) = a_0 + \sum_{n=1}^{+\infty} \sum_{m=0}^{+\infty} c_{n,m}\,\xi^m\,\exp(-n\,\lambda\,\xi), \tag{85}$$

where c_n is a coefficient. From this expression and the boundary conditions (9), it is straightforward to choose the same initial guess $F_0(\xi)$ as (19) and the same auxiliary linear operator as (20) with the same property (21).

Define

$$\kappa - 1 = \mu + \epsilon, \tag{86}$$

where $\mu \geqslant 0$ is an integer and $|\epsilon| < 1$ is a real number. Unlike in §2, the nonlinear operator $\tilde{\mathscr{N}}$ is now defined by

$$\tilde{\mathscr{N}}\,[\Phi(\xi;q)] = \kappa \left[-\frac{\partial^2 \Phi(\xi;q)}{\partial \xi^2} \right]^{\mu + \epsilon\,q} \frac{\partial^3 \Phi(\xi;q)}{\partial \xi^3} + \left(\frac{2\kappa}{\kappa + 1} \right)\,\Phi(\xi;q)\,\frac{\partial^2 \Phi(\xi;q)}{\partial \xi^2}$$
$$- \left[\frac{\partial \Phi(\xi;q)}{\partial \xi} \right]^2 - M\,\frac{\partial \Phi(\xi;q)}{\partial \xi}, \quad (87)$$

where κ is a positive real number. Then, we construct the zero-order deformation equations

$$(1-q)\,\mathscr{L}\,[\Phi(\xi;q) - F_0(\xi)] = \hbar\,q\,\exp(-l\lambda\,\xi)\,\tilde{\mathscr{N}}\,[\Phi(\xi;q)], \quad q \in [0,1], \tag{88}$$

subject to the boundary conditions (24).

The high-order deformation equation

Similarly, the solution $F(\xi)$ is given by

$$F(\xi) = F_0(\xi) + \sum_{m=1}^{+\infty} F_m(\xi), \tag{89}$$

where $F_m(\xi)$ is governed by the mth-order deformation equation

$$\mathscr{L}\,[F_m(\xi) - \chi_m\,F_{m-1}(\xi)] = \hbar\,\exp(-l\lambda\,\xi)\,\tilde{R}_m(\xi), \tag{90}$$

subject to the boundary conditions (31), where

$$\tilde{R}_m(\xi) = \frac{1}{(m-1)!}\,\frac{\partial^{m-1} \tilde{\mathscr{N}}[\Phi(\xi;q)]}{\partial q^{m-1}} \bigg|_{q=0}$$
$$= (-1)^\mu\,\kappa \sum_{n=0}^{m-1} H_{\mu,m-1-n}(\xi)\,W_n(\xi) - M\,F'_{m-1}(\xi)$$
$$+ \sum_{n=0}^{m-1} \left[\left(\frac{2\kappa}{\kappa+1} \right) F_n(\xi)\,F''_{m-1-n}(\xi) - F'_n(\xi)\,F'_{m-1-n}(\xi) \right] \tag{91}$$

using the definitions

$$H_{\mu,n}(\xi) = \frac{1}{n!} \left\{ \frac{\partial^n}{\partial q^n} \left(\frac{\partial^3 \Phi(\xi;q)}{\partial \xi^3} \left[\frac{\partial^2 \Phi(\xi;q)}{\partial \xi^2} \right]^{\mu} \right) \right\} \Bigg|_{q=0} \tag{92}$$

and

$$W_n(\xi) = \frac{1}{n!} \left\{ \frac{\partial^n}{\partial q^n} \left[-\frac{\partial^2 \Phi(\xi;q)}{\partial \xi^2} \right]^{\epsilon q} \right\} \Bigg|_{q=0}. \tag{93}$$

From the definition (92), we have

$$H_{0,n}(\xi) = F_n'''(\xi), \tag{94}$$

$$H_{1,n}(\xi) = \sum_{i=0}^{n} F_i'''(\xi) \, F_{n-i}''(\xi) = \sum_{i=0}^{n} H_{0,i}(\xi) \, F_{n-i}''(\xi), \tag{95}$$

$$H_{2,n}(\xi) = \sum_{i=0}^{n} H_{1,i}(\xi) \, F_{n-i}''(\xi), \tag{96}$$

$$\vdots$$

which gives the recursive formula

$$H_{\mu,n}(\xi) = \sum_{i=0}^{n} H_{\mu-1,i}(\xi) \, F_{n-i}''(\xi), \quad \mu \geqslant 1. \tag{97}$$

From the definition (93), we have

$$W_0(\xi) = 1,$$
$$W_1(\xi) = \epsilon \, \ln[-F_0''(\xi)],$$
$$W_2(\xi) = \frac{\epsilon \, F_1''(\xi)}{F_0''(\xi)} + \left(\frac{\epsilon^2}{2} \right) \ln^2[-F_0''(\xi)],$$
$$\vdots$$

Note that $W_n(\xi)$ for $n > 0$ can be given by

$$W_n(\xi) = \sum_{i=0}^{n-1} \left(1 - \frac{i}{n} \right) W_i(\xi) \, Z_{n-i}(\xi), \tag{98}$$

where

$$Z_n(\xi) = \frac{1}{n!} \left\{ \frac{\partial^n}{\partial q^n} \left[\epsilon \, q \, \ln \left(-\frac{\partial^2 \Phi(\xi;q)}{\partial \xi^2} \right) \right] \right\} \Bigg|_{q=0} \tag{99}$$

is easier to calculate than $W_n(\xi)$ defined by (93). Note that, from the definition (19) of $F_0(\xi)$, we have

$$\ln[-F_0''(\xi)] = \ln \lambda - \lambda \, \xi.$$

This is the reason why we choose (84) as the base functions of $F(\xi)$ for real power-law index κ. Note that when $\kappa \geqslant 1$ we can always find integer $\mu \geqslant 0$ and a real number $|\epsilon| \leqslant 1/2$ such that the expression (86) holds.

n	Homotopy-Padé approximant of $-F''(0)$
1	1.5428
2	1.5454
3	1.5447
4	1.5442
6	1.5441
8	1.5441
10	1.5441

TABLE 6. The $[n, n]$ homotopy-Padé approximant of $-F''(0)$ when $\kappa = 4/5$ and $M = 1$ with $\lambda = 3/2$.
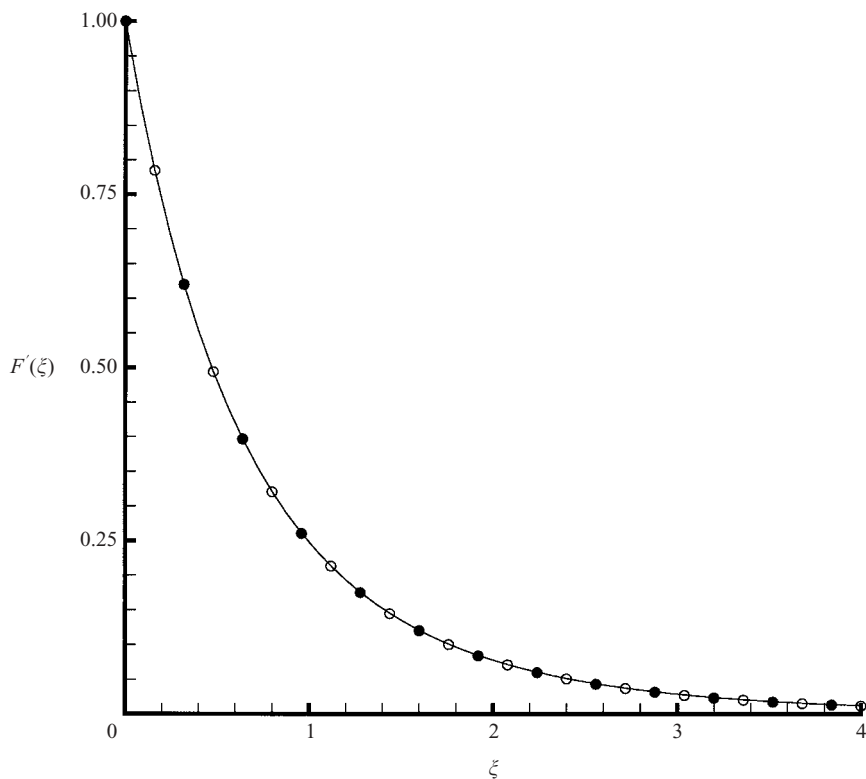

FIGURE 7. Comparison of the numerical solution with the analytic approximation of $F'(\xi)$ given by the homotopy analysis method for real κ when $\kappa = 4/5$, $M = 1$ with $\lambda = 3/2$ and $\hbar = -8/17$. Solid line: numerical solution; open circle: 10th-order analytic approximations; filled circle: 20th-order analytic approximations.

Similarly, to ensure that $F(\xi)$ can be expressed by (85) and that each coefficient $c_{m,n}$ can be modified as the order of approximation tends to infinity, we set

$$l = 0$$

in (88) and (90).

To verify the validity of the above approach for any real power-law index κ, let us first consider the case $\kappa = 1$ and $M = 1$, corresponding to $\mu = \epsilon = 0$. When $\hbar = -1/2$ and $\lambda = 2$, the corresponding homotopy-Padé approximant of $F''(0)$

	$\kappa = 4/5$		$\kappa = 3/2$		$\kappa = 4$	
M	HAM	formula (81)	HAM	formula (81)	HAM	formula (81)
0	1.028	1.037	0.982	0.971	0.989	0.981
1/2	1.308	1.312	1.131	1.126	1.046	1.041
1	1.544	1.547	1.257	1.255	1.093	1.090
3/2	1.754	1.756	1.367	1.366	1.133	1.131
2	1.945	1.947	1.466	1.465	1.167	1.167
3	2.289	2.290	1.638	1.637	1.228	1.227
5	2.874	2.875	1.918	1.918	1.322	1.322
10	4.035	4.035	2.436	2.436	1.482	1.482
25	6.517	6.517	3.428	3.428	1.752	1.752
50	9.480	9.480	4.485	4.485	2.002	2.002
75	11.835	11.835	5.259	5.259	2.167	2.167
100	13.861	13.861	5.892	5.892	2.293	2.293
250	22.989	22.989	8.478	8.478	2.750	2.750
500	33.752	33.752	11.176	11.176	3.157	3.157
750	42.265	42.265	13.140	13.140	3.423	3.423
1000	49.581	49.581	14.741	14.741	3.625	3.625

TABLE 7. The comparison of the analytic results for $-F''(0)$ given by the proposed homotopy analysis method (HAM) when $\kappa = 4/5, \kappa = 3/2$ and $\kappa = 4$ with those given by the analytic formula (81).

converges quickly to the exact analytic result $F''(0) = -\sqrt{2}$. The corresponding 10th-order approximation of $F'(\xi)$ agrees well with the exact analytic solution $F'(\xi) = \exp(-\sqrt{2}\,\xi)$. Then, we reconsider the case of $\kappa = 2$ and $M = 1$ and it is found that the analytic approach proposed in this section gives a convergent result (with $\lambda = 5/4$ and $\hbar = -4/7$), and the homotopy-Padé approximant of $F''(0)$ converges quickly to the numerical result -1.187 given by Andersson *et al.* (1992). Finally, we consider the case of $M = 1$ and $\kappa = 4/5$, a real power-law index. The convergent results are obtained when $\lambda = 3/2$ and $\hbar = -8/17$, and the homotopy-Padé approximant of $F''(0)$ converges quickly to the numerical result -1.544 given by the Andersson *et al.* (1992), as shown in table 6. The corresponding 10th- and 20th-order approximations of $F'(\xi)$ agree well with the numerical result given by the Runge–Kutta method with $F''(0) = -1.5441$, as shown in figure 7. All of these verify the validity of the analytic approach for any real power-law index κ proposed in this section.

In most cases, convergent results can be obtained by choosing λ and $\hbar$ as defined by (82) and (83), although, for M less or a little more than 2, a negative value of $\hbar$ had to be chosen closer to zero. All of our computations verify that

(*a*) the convergence regions can be enlarged as the auxiliary parameter $\hbar$ tends to zero from below;

(*b*) the convergence rate and region of $F''(0)$ are greatly increased by the homotopy-Padé technique.

The analytic results for $F''(0)$ given by the proposed approach in a large range $0 \leqslant M \leqslant 1000$ for the integer power-law index $\kappa = 4$ and the real power-law index $\kappa = 4/5$ and $\kappa = 3/2$ are listed in table 7, compared with those given by the formula (81). It is interesting that the analytic formula (81) gives good approximations of $F''(0)$ even for real power-law index κ, as shown in figure 8. So, we are quite sure that (81) is an accurate approximation of the dimensionless velocity gradient $F''(0)$ for real power-law index $\kappa > 0$ and magnetic field parameter $0 < M < +\infty$. Thus, using
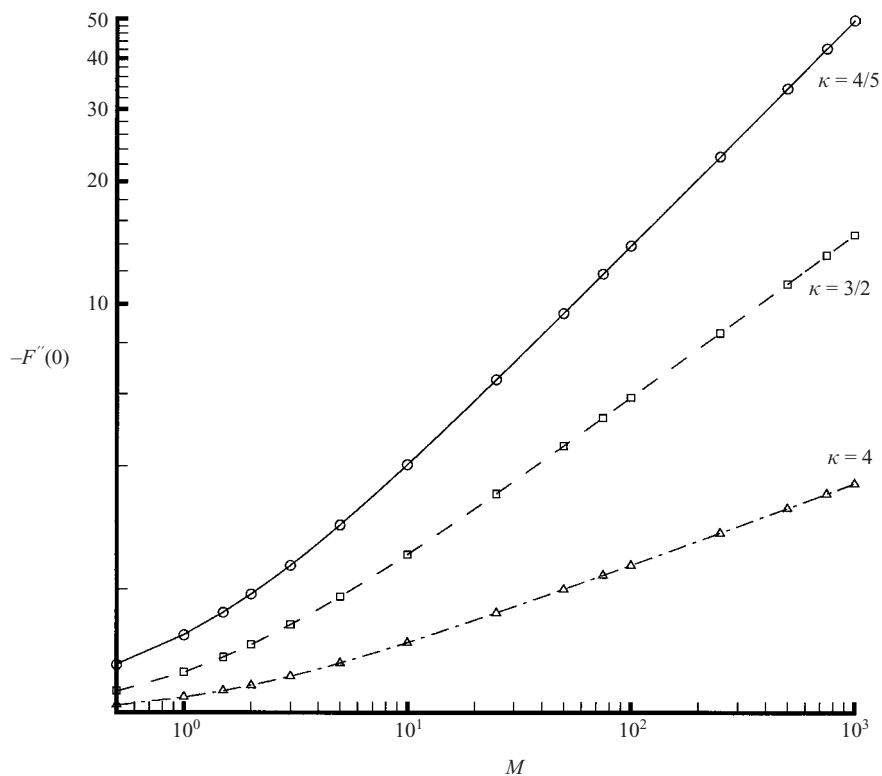
FIGURE 8. Comparison of $F''(0)$ given by (81) with the numerical results. Solid line: result given by (81) when $\kappa = 4/5$; dashed line: result given by (81) when $\kappa = 3/2$; dash-dotted line: result given by (81) when $\kappa = 4$; open circle: the numerical solution when $\kappa = 4/5$; square: the numerical solution when $\kappa = 3/2$; triangle: the numerical solution when $\kappa = 4$.

(81) and the definition (10), we can calculate the skin friction on the sheet accurately enough for practical applications in engineering.

Based on numerical results for $0.4 \leqslant \kappa \leqslant 2$ and $0 \leqslant M \leqslant 2$, Andersson *et al.* (1992) found that $-F''(0)$ increases monotonically with M for a given fluid but decreases monotonically with κ for a given magnetic field. The analytic expression (81) indicates that this finding can be expanded to include non-Newtonian fluids with any real power-law index $\kappa > 0$ and any magnetic field parameter $0 < M < +\infty$, as shown by figures 6 and 8. Physically, it indicates that the effect of the non-Newtonian nature of the fluid is to reduce the skin friction, and that the effect of the magnetic field is to increase the skin friction.

4. Discussion and conclusion

In this paper the homotopy analysis method is employed to give analytic solutions of the magnetohydrodynamic viscous flows of non-Newtonian fluids over a stretching sheet. For the so-called second-order ($\kappa = 2$) and third-order ($\kappa = 3$) power-law fluids the explicit analytic solutions are expressed by recursive formulas of constant coefficients, which can be regarded as the definition of the solution of the nonlinear differential equations (8) and (9) when $\kappa = 2$ and $\kappa = 3$. Also, for real power-law index $\kappa > 0$ and magnetic field parameter M in a quite large range we propose an

analytic approach. All of our analytic results agree well with the numerical ones. In particular, a rather simple analytic formula for the dimensionless velocity gradient at the wall is found, which is quite accurate for real power-law index $\kappa > 0$ and magnetic field parameter $0 < M < +\infty$. This analytic formula (81) can give an accurate enough skin friction result on the moving sheet to find wide applications in the metallurgy industry. Physically, it indicates that the magnetic field tends to increase the wall friction, and that this effect is more pronounced for shear-thinning ($\kappa < 1$) than for shear-thickening ($\kappa > 1$) fluids.

This paper also verifies that the homotopy analysis method is valid for complicated, strongly nonlinear problems in fluid mechanics.

REFERENCES

ADOMIAN, G. 1976 Nonlinear stochastic differential equations. *J. Math. Anal. Applic.* **55**, 441–452.

ADOMIAN, G. 1994 *Solving Frontier Problems of Physics: The Decomposition Method*. Kluwer.

ALEXANDER, J. C. & YORKE, J. A. 1978 The homotopy continuation method: numerically implementable topological procedures. *Trans. Am. Math. Soc.* **242**, 271–284.

ANDERSSON, H. I. 1992 MHD flow of a viscous fluid past a stretching surface. *Acta Mechanica* **95**, 227–230.

ANDERSSON, H. I. 1995 A exact solution of the Navier-Stokes equations for magnetohydrodynamics flow. *Acta Mechanica* **113**, 241–244.

ANDERSSON, H. I., BECH, K. H. & DANDAPAT, B. S. 1992 Magnetohydrodynamic flow of a power-law fluid over a stretching sheet. *Intl J. Non-Linear Mech.* **27**, 929–936.

ANDERSSON, H. I. & DANDAPAT, B. S. 1991 Flow of a power-law fluid over a stretching sheet. *Stability Appl. Anal. Continuous Media* **1**, 339–347.

AWREJCEWICZ, J., ANDRIANOV, I. V., & MANEVITCH, L. I. 1998 *Asymptotic Approaches in Nonlinear Dynamics*. Springer.

CHAKRABARTI, A. & GUPTA, A. S. 1979 Hydromagnetic flow and heat transfer over a stretching sheet. *Q. Appl. Maths* **37**, 73–78.

CHAN, T. F. C. & KELLER, H. B. 1982 Arc-length continuation and multi-grid techniques for nonlinear elliptic eigenvalue problems. *SIAM J. Sci. Statist. Comput.* **3**, 173–193.

COLE, J. D. 1958 *Perturbation Methods in Applied Mathematics*. Blaisdell.

CRANE, L. J. 1970 Flow past a stretching plate. *Z. Angew. Math. Phys.* **21**, 645–647.

DANDAPAT, B. S. & GUPTA, A. S. 1989 Flow and heat transfer in a viscoelastic fluid over a stretching sheet. *Intl J. Non-Linear Mech.* **24**, 215–219.

DINAR, N. & KELLER, H. B. 1985 Computations of taylor vortex flows using multigrid continuation methods. *Tech. Rep.* California Institute of Technology.

DJUKIC, D. S. 1973 On the use of Crocco's equation for the flow of power-law fluids in a transverse magnetic field. *AIChE J.* **19**, 1159–1163.

DJUKIC, D. S. 1974 Hiemenz magnetic flow of power-law fluids. *Trans. ASME: J. Appl. Mech.* **41**, 822–823.

ERICKSON, L. E., FAN, L. T. & FOX, V. G. 1966 Heat and mass transfer on a moving continuous flat plate with suction or injection. *Ind. Engng Chem. Fundam.* **5**, 19–25.

GRIGOLYUK, E. E. & SHALASHILIN, V. I. 1991 *Problems of Nonlinear Deformation: The Continuation Method Applied to Nonlinear Problems in Solid Mechanics*. Kluwer.

HILTON, P. J. 1953 *An introduction to homotopy theory*. Cambridge University Press.

HINCH, E. J. 1991 *Perturbation Methods*. Cambridge University Press.

KARMISHIN, A. V., ZHUKOV, A. I. & KOLOSOV, V. G. 1990 *Methods of dynamics calculation and testing for thin-walled structures*. Mashinostroyenie, Moscow (in Russian).

Liao, S. J. 1992 The proposed homotopy analysis technique for the solution of nonlinear problems. PhD thesis, Shanghai Jiao Tong University.

Liao, S. J. 1999a An explicit, totally analytic approximation of Blasius viscous flow problems. *Intl J. Non-Linear Mech.* **34**, 759–778.

Liao, S. J. 1999b A uniformly valid analytic solution of 2D viscous flow past a semi-infinite flat plate. *J. Fluid Mech.* **385**, 101–128.

Liao, S. J. 2002 An analytic approximation of the drag coefficient for the viscous flow past a sphere. *Intl J. Non-Linear Mech.* **37**, 1–18.

Liao, S. J. 2003a An analytic approximate technique for free oscillations of positively damped systems with algebraically decaying amplitude. *Intl J. Non-Linear Mech.* **38**, 1173–1183.

Liao, S. J. 2003b An explicit analytic solution to the Thomas-Fermi equation. *Appl. Maths Comput.* (to appear).

Liao, S. J. & Campo, A. 2002 Analytic solutions of the temperature distribution in Blasius viscous flow problems. *J. Fluid Mech.* **453**, 411–425.

Liao, S. J. & Cheung, K. F. 2003 Homotopy analysis of nonlinear progressive waves in deep water. *J. Engng Maths* **45**, 105–116.

Liao, S. J. & Chwang, A. T. 1998 Application of homotopy analysis method in nonlinear oscillations. *Trans. ASME: J. Appl. Mech.* **65**, 914–922.

Lyapunov, A. M. 1892 *General problem on stability of motion*. English transl. Taylor & Francis, London, 1992.

McCormack, P. D. & Crane, L. J. 1973 *Physical Fluid Dynamics*. Academic.

McLeod, J. B. & Rajagopal, K. R. 1987 On the uniqueness of flow of a Navier-Stokes fluid due to a stretching boundary. *Arch. Rat. Mech. Anal.* **98**, 385–393.

Murdock, J. A. 1991 *Perturbations: Theory and Methods*. John Wiley & Sons.

Nayfeh, A. H. 2000 *Perturbation Methods*. John Wiley & Sons.

Pavlov, K. B. 1974 Magnetohydrodynamic flow of an impressible viscous fluid caused by deformation of a surface. *Magnitnaya Gidrodinamika* **4**, 146–147.

Rajagopal, K. R., Na, T. Y. & Gupta, A. S. 1984 Flow of a viscoelastic fluid over a stretching sheet. *Rheol. Acta* **24**, 213–215.

Rajagopal, K. R., Na, T. Y. & Gupta, A. S. 1987 A non-similar boundary layer on a stretching sheet in a non-Newtonian fluid with uniform free stream. *J. Math. Phys. Sci.* **21**, 189–200.

Sakiadis, B. C. 1961 Boundary layer behavior on continuous solid surface. *AIChE. J.* **7**, 26–28.

Sarpkaya, T. 1961 Flow of non-Newtonian fluids in a magnetic field. *AIChE. J.* **7**, 324–328.

Takhar, H. S., Raptis, A. A. & Perdikis, A. A. 1987 MHD asymmetric flow past a semi-infinite moving plate. *Acta Mechanica* **65**, 287–290.

Troy, W. C., Overman, E. A., Ermentrout, G. B. & Keener, J. P. 1987 Uniqueness of flow of a second-order fluid past a stretching surface. *Q. Appl. Math.* **44**, 753–755.

Vajravelu, K. 1986 Hydromagnetic flow and heat transfer over a continuous, moving, porous, flat surface. *Acta Mechanica* **64**, 179–185.

Van Dyke 1975 *Perturbation Methods in Fluid Mechanics*. The Parabolic Press.

Wang, C., Zhu, J. M., Liao, S. J. & Pop, I. 2003 On the explicit analytic solution of Cheng-Chang equation. *Intl J. Heat Mass Transfer* **46**, 1855–1860.